



SERVICE  
ALTIMÉTRIE  
&  
LOCALISATION  
PRÉCISE



SALP

## Hy-2A: Global statistical assessment and cross-calibration with Jason-2 over Ocean

Reference: SALP-NT-M-EA-22364-CLS  
Nomenclature: CLS-DOS-NT-14-148  
Issue: 1.0  
Date: 2014, Sep.01

CLS (siège)  
8-10 rue Hermès  
Parc technologique du Canal  
31520 Ramonville Saint-Agne  
FRANCE

Tél. : +33 (0)5 61 39 47 00  
Fax : +33 (0)5 61 75 10 14  
Mél. : [info@cls.fr](mailto:info@cls.fr)  
Web : [www.cls.fr](http://www.cls.fr)

CLS Brest Le Ponant  
Avenue La Pérouse  
29280 Plouzané  
FRANCE

Tél. : +33 (0)2 98 05 76 80  
Fax : +33 (0)2 98 05 76 90






### Chronology Issues:

Issue:	Date:	Reason for change:	Author
1.0	01/09/2014	First version of the document	Matthias Raynal

### People involved in this issue:

Written by (*):	M Raynal	2014, Sept 8	
Checked by (*):	S. d'Alessio	2014, Sept 8	
Approved by (*):		Date + Initial:( visa or ref)	
Application authorized by (*):	JM. Lachiver	2014, Sept 01	

*\*In the opposite box: Last and First name of the person + company if different from CLS*

### Index Sheet:

Context:	
Keywords:	Hy-2A, performance, cross-calibration, DUACS
Hyperlink:	

### Distribution:

Company	Means of distribution	Names
CLS	Notification	



## List of tables and figures

### List of tables:

Table 1: List of the geophysical corrections used to estimate the Sea Surface Height for HY-2A and Jason-2 .....	2
Table 2: List of HPP outputs available in RS-IGDR products .....	3

### List of figures:

Figure 1: Percentage of missing measurements over ocean for HY-2A (left panel) and for Jason-2 (right panel).....	3
Figure 2: Daily percentage of missing measurements for HY-2A and Jason-2 over ocean .....	4
Figure 3: Daily percentage of edited measurements for HY-2A and Jason-2 over all surfaces (left panel) and over ocean (right panel) .....	5
Figure 4: Map of the percentage of valid measurements over ocean for HY-2A (left panel) and for Jason-2 (right panel).The values has been computed over 1cycle for each mission. ....	5
Figure 5: Temporal evolution of the daily mean (left panel) and standard deviation (right panel) of mispointing derived from waveforms for HY-2A and Jason-2.....	6
Figure 6: distribution in percentage of data of backscatter coefficient values for HY-2A and Jason-2 (left panel). Temporal evolution of the daily mean of backscatter coefficient for HY-2A and Jason-2 (right panel) .....	7
Figure 7: Map of along track Sigma0 differences between HY-2A and Jason-2 over the 3 months available .....	7
Figure 8: Temporal evolution of the daily mean (left panel) and standard deviation (right panel) of significant wave height for HY-2A and Jason-2 .....	8
Figure 9: Map of along track Significant Wave Height differences between HY-2A and Jason-2 over the 3 months available. ....	8
Figure 10: Sea Level Anomaly power spectra computed over HY-2A's cycle 53 with NSOAS SSB (red curve), one parameter SSB (blue curve) and Jason-2 SLA (green curve) computed over the same period. ....	9
Figure 11: 20Hz non corrected Sea Surface Height power spectra computed over HY-2A cycle 54 for HY-2A (black curve) and Jason-2 (gray curve) .....	10
Figure 12: Temporal evolution of the daily mean (left panel) and standard deviation (right panel) of sea level anomaly for HY-2A and Jason-2. The HY-2A SLA has been align on Jason-2 SLA at the beginning of the time series to facilitate the figure interpretation ....	10
Figure 13: Map of along track Sea Level Anomaly differences between HY-2A and Jason-2 over the 3 months available .....	11
Figure 14: Cycle by cycle standard deviation of the SSH differences at crossovers for HY-2A and Jason-2. ....	12
Figure 15: Cycle by cycle mean of SSH differences forHY-2A, Jason-2 and Cryosat-2 mono-mission analyses. ....	12
Figure 16: Map of the mean SSH differences at crossovers for HY-2A (left panel) and Jason-2 (right panel) over the 3 months available. ....	13
Figure 17: Map of the mean SSH differences at crossovers for HY-2A when datation bias correction is applied .....	13
Figure 18: Map of the mean SSH differences between HY-2A and Jason2 at crossovers over the 3 months available. ....	14



Figure 19: Temporal evolution of the daily mean (left panel) and standard deviation (right panel) of sea level anomaly for HY-2A and Jason-2. ....	15
Figure 20: Map of the mean SSH differences at crossovers for HY-2A over the 3 months available. ....	15
Figure 21: Map of the mean SSH differences at crossovers between HY-2A and Jason-2 over the 3 months available. ....	16

## Liste des AC et AD

### Liste des AC :

Aucune entrée de table des matières n'a été trouvée.

### Liste des AD :

Aucune entrée de table des matières n'a été trouvée.

## Applicable documents

AD 1 Marché CNES 104685/00

AD 2 Devis 104685-16-79 : Exploitation du HPP (HY-2A Processing Prototype) et des produits RS-IGDR dans DUACS pour l'année 2014 - SALP-BC-M-EA-22317-CLS

## Reference documents

RD 1 Bon de commande n° 4500045835 1 DCT091 sur marché n° 104685/00

RD 2 [Picot et al., 2013]: N. Picot, J-C. Poisson, J-F. Legeais, A. Vernier, P. Thibaut, J-M. Lachiver, J. Lambin, "Towards an Operational Use of HY-2A in SSALT/Duacs: Evaluation of the Altimeter Performances Using NSOAS S-IGDR Data", OSTST 2013

RD 3 [Iijima et al, 1999] : "Automated daily process for global ionospheric total electron content maps and satellite ocean altimeter ionospheric calibration based on Global Positioning System data B.A", Journal of Atmospheric and Solar-Terrestrial Physics 61 (1999) 1205-1218

RD 4 [Mertz et al., 2009]: F. Mertz, G. Dibarboue, E. Bronner, P-Y. le Traon, "SSALTO/DUACS: Innovative Method To Reduce The Orbit Error Simultaneously On Several Satellites."

RD 5 [Dibarboue et al., 2013]: G. Dibarboue, F. Boy, J-D. Desjonqueres, S. Labroue, Y. Lasne, N. Picot, J-C Poisson, P. Thibaut, « Investigating short wavelength correlated errors on low-resolution mode altimetry"

RD 6 [Molteni et al, 1996]: Molteni, F., Buizza, R., Palmer, T. N. and Petroliagis, T., "The ECMWF Ensemble Prediction System: Methodology and validation", Q. J. R. Meteorol. Soc., 122: 73-119. doi: 10.1002/qj.49712252905



## List of Contents

<b>1. INTRODUCTION.....</b>	<b>1</b>
<b>1.1. Purpose and scope .....</b>	<b>1</b>
<b>1.2. Document structure.....</b>	<b>1</b>
<b>2. Processing and data coverage.....</b>	<b>1</b>
<b>2.1. Processing.....</b>	<b>1</b>
<b>2.2. Data coverage .....</b>	<b>3</b>
2.2.1. Missing measurements.....	3
2.2.2. Valid Measurements.....	4
<b>3. Analysis of altimeter parameters.....</b>	<b>5</b>
<b>3.1. Apparent Squared Mispointing from Waveforms.....</b>	<b>6</b>
<b>3.2. Backscatter Coefficient (Sigma0).....</b>	<b>6</b>
<b>3.3. Significant Wave Height (SWH).....</b>	<b>7</b>
<b>3.4. Sea State Bias.....</b>	<b>8</b>
<b>4. Sea level performances .....</b>	<b>9</b>
<b>4.1. Analysis of along-track Sea Level Anomalies .....</b>	<b>9</b>
4.1.1. High frequency content .....	9
4.1.2. Temporal evolution .....	10
4.1.3. Correlated geographical biases with Jason-2 .....	11
<b>4.2. Analysis of Sea Surface Height Crossovers Differences .....</b>	<b>11</b>
4.2.1. Mono mission crossovers .....	11
4.2.2. Multi-mission crossovers: HY-2A / Jason-2.....	13
<b>5. Impact in DUACS .....</b>	<b>14</b>
<b>5.1. Orbit error correction .....</b>	<b>14</b>
<b>5.2. Temporal evolution of SLA.....</b>	<b>14</b>
<b>5.3. Mono-mission crossovers .....</b>	<b>15</b>
<b>5.4. Multi-mission crossovers .....</b>	<b>15</b>
<b>6. Conclusion .....</b>	<b>16</b>
<b>Appendix A - List of acronyms .....</b>	<b>17</b>
<b>Appendix B - ANNEXES .....</b>	<b>18</b>



## 1. INTRODUCTION

This document is an output of CLS activity performed in the framework of CNES/CLS SALP contract (AD 1 and AD 2, order form RD 1).

### 1.1. Purpose and scope

HY-2A is the first altimetry and radiometry satellite of the China National Space Administration (CNSA), it was successfully launched on 15<sup>th</sup> of August 2011.

The National Satellite Ocean Application Service (NSOAS) is responsible for the ground segment and for distributing collected data and HY-2A L2 products. The French contribution performed by the Centre National d'Etudes Spatiales (CNES) on this project consists mainly in supplying the orbit computed from DORIS, GPS and laser measurements. In addition CNES has conducted several analyses in order to analyze the feasibility of HY2 L2 data inside the DUACS multi mission system.

A first assessment was performed in November 2012 (Picot et al, 2013, RD 2) over 2 complete cycles provided by NSOAS. Results showed that NSOAS products data quality was lower than expected. Indeed the comparison of HY-2A S-IGDR retracked parameters with Jason-2 pointed out quite large differences. In 2013 an agreement has been reached between NSOAS and CNES, consisting on using NSOAS products waveforms (S-IGDR products) to apply a MLE4 retracking developed by CNES and then to send back re-processed products (RS-IGDR products) to the NSOAS. This process has been called HY-2A Processing Prototype (HPP).

After validation of the HPP and the assessment of RS-IGDR products, the data quality has been estimated sufficient to integrate them in the DUACS system. Since beginning of June 2014 HY-2A RS-IGDR products have been used in DUACS to provide near real time and differed time multi-mission products (<http://www.aviso.altimetry.fr/en/data/product-information/information-about-mono-and-multi-mission-processing/ssaltoduacs-multimission-altimeter-products.html>).

This technical note aims at describing improvement performed to enhanced S-IGDR products and analyzing the global quality of RS-IGDR products. To achieve this goal, mono-mission metrics and comparisons with Jason-2 over the same period are presented.

### 1.2. Document structure

This document is structured into an introductory chapter followed by four chapters describing:

- The data used and the data coverage (missing and valid measurements).
- The analysis of HPP outputs (altimeter parameters).
- The assessment of HY-2A global performances.
- The assessment of HY-2A global performances in DUACS

## 2. Processing and data coverage

### 2.1. Processing

In this study RS-IGDR data are used for cycle 67 to 72, which corresponds to slightly less than three months (12 April 2014 to 5 July 2014). This is an homogeneous dataset produced with HPP version 3.1.

Today, only parameters derived from the Ku band altimeter are computed in the HPP. The HPP outputs, altimeter range, significant wave height (SWH), backscatter coefficient (sigma-0) and mispointing (KSI2) are obtained using a MLE4 retracking applied on S-IGDR waveforms, knowing that instrument internal calibrations are not available on CNES side. We used these RS-IGDR parameters in our study.

Proprietary information: no part of this document may be reproduced divulged or used in any form without prior permission from CNES.



As we have detected inconsistent orbit values in S-IGDR products (probably due to an inadequate interpolation method used on NSOAS side), we also update this parameter in the HPP. Sea Level Anomaly (SLA) is computed using the following formula:

$$SLA = Orbit\ altitude - Altimeter\ Range - \Sigma IC - \Sigma GC - MSS$$

where:

*IC* = Instrumental Corrections

*GC* = Geophysical Corrections

*MSS* = Mean Sea Surface

The HY-2A satellite is equipped with a microwave radiometer, however the radiometer wet troposphere correction in S-IGDR products is of poor quality.. Therefore we chose to apply the wet troposphere correction derived from the ECMWF model (European Centre for Medium-range Weather Forecasts) (Molteni et al., 1996, RD 6). Same observations have been made with the ionosphere correction derived from dual band frequency of the HY-2A altimeter. Values given in S-IGDR products are of poor quality, so we chose to use Global Ionosphere Maps (GIM) model (Iijima et al, RD 3).

Concerning the instrumental corrections we apply the Doppler correction, the internal path delay and the center of mass provided in S-IGDR products.

Comparisons of S-IGDR Sea Surface Bias (SSB) (computed with S-IGDR SWH and wind speed) with Jason-2 SSB showed discrepancies. These anomalies and the RS-IGDR SSB computation are detailed in paragraph 3.4.

When compared to Jason-2, we use for the two satellites exactly the same geophysical corrections derived from models. In this way we only assess HY-2A altimeter performances and radial orbit performances (and not geophysical corrections differences). Geophysical corrections are described in Table 1, other parameters assessed in this study are described in Table 2

#### Geophysical Corrections applied to HY-2A and Jason-2 (in this study)

Dry troposphere correction	ECMWF model
Wet troposphere correction	ECMWF model
Dynamical atmospheric correction	high resolution Mog2D model (Carrere and Lyard, 2003)
Ionospheric correction	GIM model
Ocean tide	GOT4.8 model (Ray, 1999)
Solid earth tide	elastic response to tidal potential (Cartwright and Edden, 1973)
Pole tide	(Wahr, 1985)

Table 1: List of the geophysical corrections used to estimate the Sea Surface Height for HY-2A and Jason-2






---

**HY-2A RS-IGDR parameters**

Orbit	CNES MOE-C standards
Sea State Bias	HY-2A: one parameter SSB depending on SWH / Jason-2: non-parametric (Tran et al., 2010)
Range, SWH, Sigma0, Ksi2	MLE4 retracking

Table 2: List of HPP outputs available in RS-IGDR products

---

## 2.2. Data coverage

The data coverage is impacted by missing measurements and also spurious sea level estimations. In this part, we analyze separately the impact of both issues.

### 2.2.1. Missing measurements

The percentage of missing measurements can be affected by several events such as special calibration, acquisition station problems or missing telemetry. This parameter is monitored using theoretical passes.

Figure 1 shows the percentage of missing measurements over ocean for one HY-2A cycle (14 days) and for one Jason-2 cycle (10 days). Over open ocean the percentage of missing measurements is quite similar for both missions. For HY-2A we notice missing measurements for several parts of 8 passes. To explain their origins (calibration, telemetry, reception station ...), NSOAS information would be necessary.

For high latitudes, differences are much higher and are correlated with the presence of sea ice. In this case the number of available measurements could be impacted by the high reflectivity of ice surface and the different behavior of onboard tracking algorithms (on specular surfaces, backscattered wave power is much higher so an adapted tracker method should be used to position correctly the acquisition window). During the cycle 62 (not shown here) we observed a strong change of the Automatic Gain Control value correlated with a higher percentage of available measurements for high latitudes.

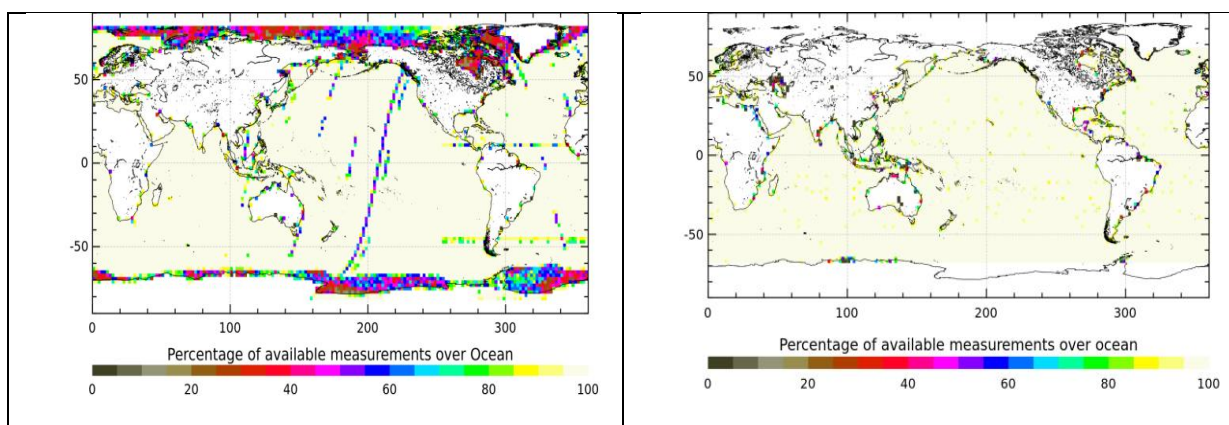


Figure 1: Percentage of missing measurements over ocean for HY-2A (left panel) and for Jason-2 (right panel)

The temporal evolution of missing measurements is presented Figure 2. The daily number of missing measurements over ocean is much higher for HY-2A (11.9 % in average) than for Jason-2 (0.08 % in average). The variability of this parameter is also higher for HY-2A. We notice that an important





part (around 9 %) of missing measurements are located at high latitudes (above  $60^\circ$ ), as it was showed Figure 1.

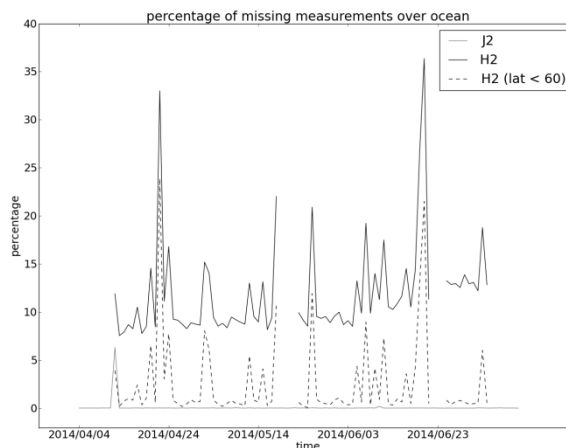


**Figure 2: Daily percentage of missing measurements for HY-2A and Jason-2 over ocean**

Over ocean and for latitudes lower than  $60^\circ$  the percentage of available measurements (97.4 %) is acceptable as the main part of missing measurements is not related to HY-2A altimeter accuracy (when over ocean, entire passes are missing this is probably related to a ground segment operation).

For information (not shown here) the percentage of missing measurements over land is quite high. To give an idea of the magnitude, this percentage over land for HY-2A is similar with the Jason-1 one.

### 2.2.2. Valid Measurements

In order to calculate the sea level estimations, corrupted measurements have to be removed, especially in regions impacted by rain cells and sea ice or in coastal areas. In the case of this study we applied a specific editing dedicated to open ocean analysis. This editing is based on a threshold validation applied on different parameters (geophysical correction, retracked parameters and Sea Level Anomaly). More information on the thresholds values can be found in Jason-2 annual reports.

The daily percentage of edited measurements (Figure 3) is quite similar for Jason-2 and HY-2A. Over all kind of surfaces, for Jason-2, this percentage increases with ice covering, whereas it stays constant for HY-2A since much more measurements are missing for high latitudes.

Over ocean, several days with high values of this percentage appears for the HY-2A mission, it occurs when entire passes are edited.

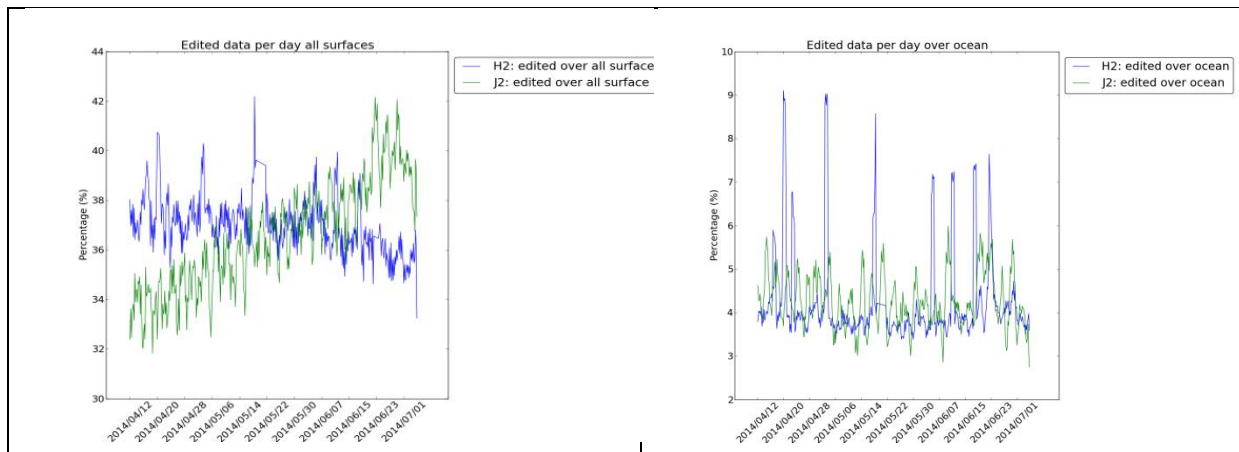


**Figure 3: Daily percentage of edited measurements for HY-2A and Jason-2 over all surfaces (left panel) and over ocean (right panel)**

The spatial representation of valid measurements (Figure 4) shows that in the equatorial band, where the humidity content is high, same areas for HY-2A and Jason-2 present edited measurements. The main part of edited measurements in this area is removed by thresholds on 20Hz noise. We also notice a large band of edited measurements for HY-2A at 50° south of latitude. In this band, around 20 % of available measurements are edited due to inconsistent values of the Doppler correction. Indeed, we noticed that for several measurements in this latitudes band, the Doppler correction has been set to 0.0 m while it should be around +/- 10 cm (value estimated as function of radial velocity).

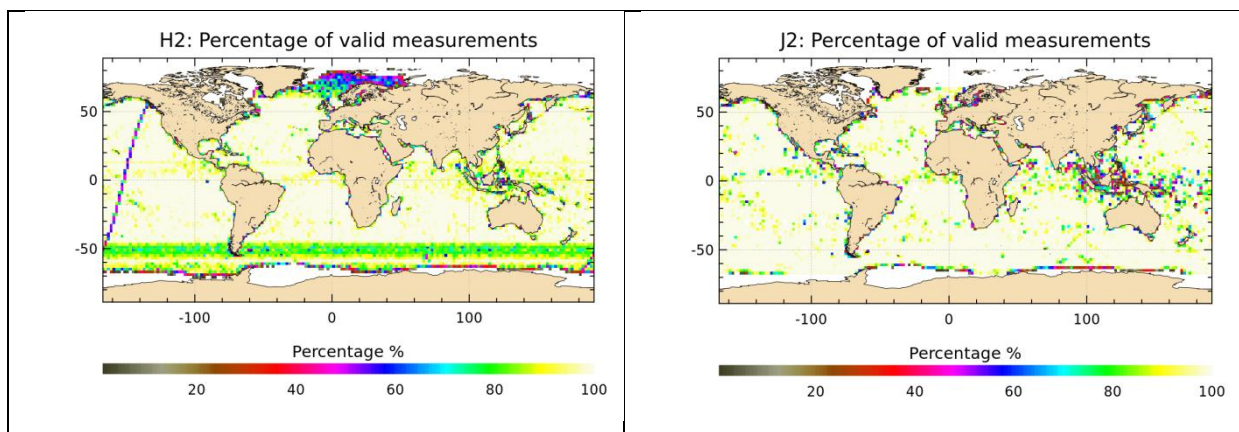


**Figure 4: Map of the percentage of valid measurements over ocean for HY-2A (left panel) and for Jason-2 (right panel). The values has been computed over 1cycle for each mission.**

To conclude, over open ocean the number of edited measurement is quite similar between HY-2A and Jason-2. Today 20 % of available measurements are edited because of the Doppler correction. By computing this instrumental correction in the HPP, the number of edited measurement could be reduce in this band of latitude.

### 3. Analysis of altimeter parameters

The analysis of retracked parameters is presented in this chapter. It allows us to highlight any unusual event or HY-2A altimeter. Note that the altimetric distance assessment is described in next chapter (Sea level performances). It is also important to notice that around the 18<sup>th</sup> of May we didn't receive S-IGDR products from the NSOAS since HY-2A was in survival mode due to an abnormal rotation of the scatterometer.



### 3.1. Apparent Squared Mispointing from Waveforms

The off nadir angle (mispointing angle) is an information estimated from the trailing edge of waveforms. Figure 5 displays daily average and daily standard deviation of this parameter for HY-2A and Jason-2.

The HY-2A mispointing (square value) is around  $0.2 \text{ deg}^2$ , it was stable at the beginning but presents fluctuations since end of April 2014. The HY-2A mispointing daily average is higher and less monotone than Jason-2's mispointing but the standard deviation of this parameter shows that HY-2A mispointing is twice less noisy than for Jason-2.

It seems that the mispointing fluctuations don't impact the data quality since we do not observe correlation with the evolution of other parameters. This is indeed in line with the MLE4 retracking performances that allow accounting for mispointing angles up to 0.7 degrees.

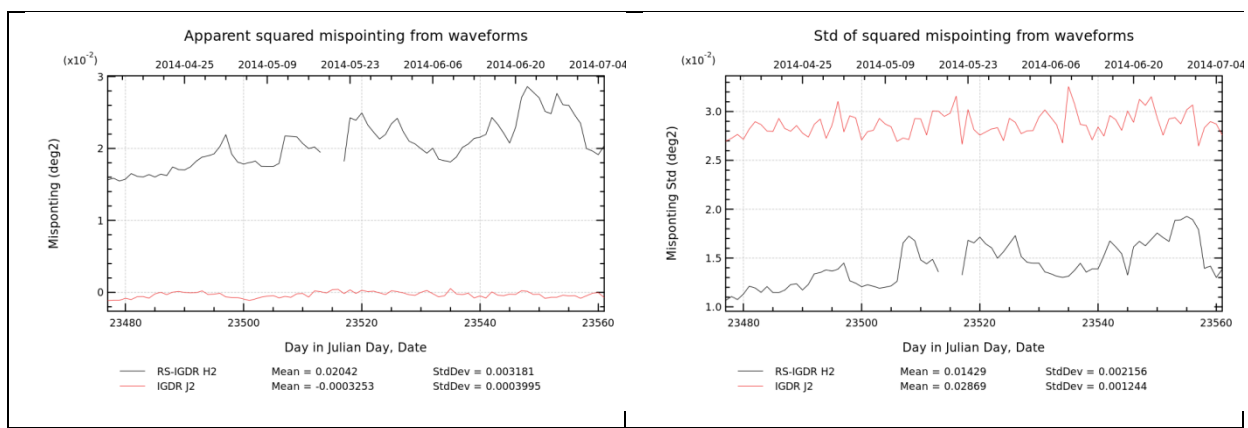


Figure 5: Temporal evolution of the daily mean (left panel) and standard deviation (right panel) of mispointing derived from waveforms for HY-2A and Jason-2

### 3.2. Backscatter Coefficient (Sigma0)

The analysis of the sigma-0 parameter quality indicates differences with Jason-2.

Firstly, the distributions of backscatter coefficients are different for HY-2A and Jason-2. Left panel of the Figure 6 shows a 1.86 dB bias. HY-2A sigma0 distribution corrected for this bias value matches pretty well the Jason-2 sigma0 distribution.

Secondly, a drift is detected on the Sigma-0 daily mean (right panel of Figure 6). This drift of about 0.5 dB is produced by a strong evolution of the sigma-0 in May 2014. At the time of writing this abnormal behaviour of HY2 sigma0 is not explained. It could be due to instrument evolutions not taken into account in the current HPP processing (mainly PTR evolution). NSOAS information would be necessary to further analyze this behavior.

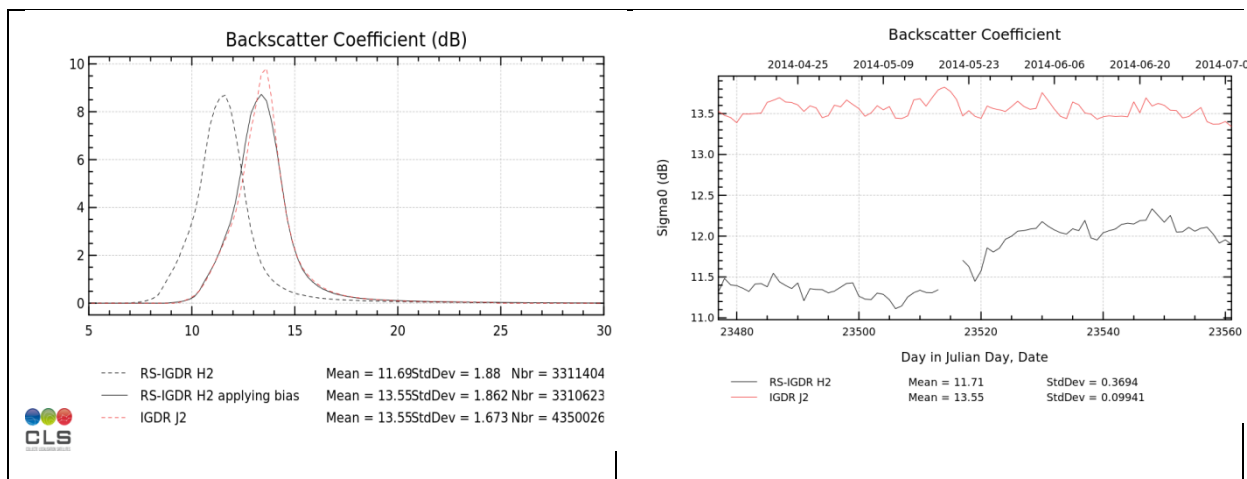


**Figure 6: distribution in percentage of data of backscatter coefficient values for HY-2A and Jason-2 (left panel). Temporal evolution of the daily mean of backscatter coefficient for HY-2A and Jason-2 (right panel)**

The map of Sigma0 differences (Figure 7) with Jason-2 shows that main differences are observed in Indonesia where rain cells are often present during this season. In other part of the ocean, the variations of sigma0 differences do not highlight abnormal behaviour. Map of Sigma0 differences between Altika/Jason-2 and Cryosat-2/Jason-2 are presented in Annexes. We observe for the Indonesian area the same kind of pattern between Altika and Jason-2 but results should be carefully interpreted since Altika altimeter is more sensitive to the humidity content (Ka band). The comparison between Cryosat-2 and Jason-2 shows more variability in this area and same kind of patterns over open-ocean.

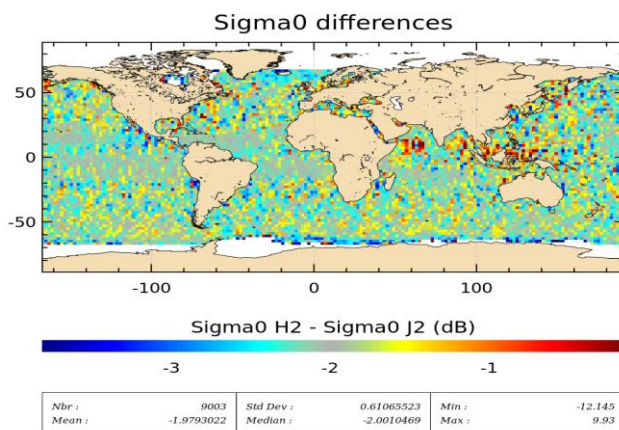


**Figure 7: Map of along track Sigma0 differences between HY-2A and Jason-2 over the 3 months available**

To conclude, the HY-2A sigma0 shape is very close to the Jason-2 sigma0. The drift of HY-2A sigma0 should be monitored, for the moment it does not impact SLA estimations since we perform a one order SSB as function of SWH only. However this strong evolution does not allow to compute reliable wind speed value.

### 3.3. Significant Wave Height (SWH)

The HY-2A and Jason-2 significant wave height temporal evolutions are very close whereas the spatial and temporal samplings are not the same. Figure 8 shows that compared to Jason-2, HY-2A SWH are in average overestimated of 0.5 cm only. Standard deviations are also very close which traduces the good quality of HY-2A altimeter.

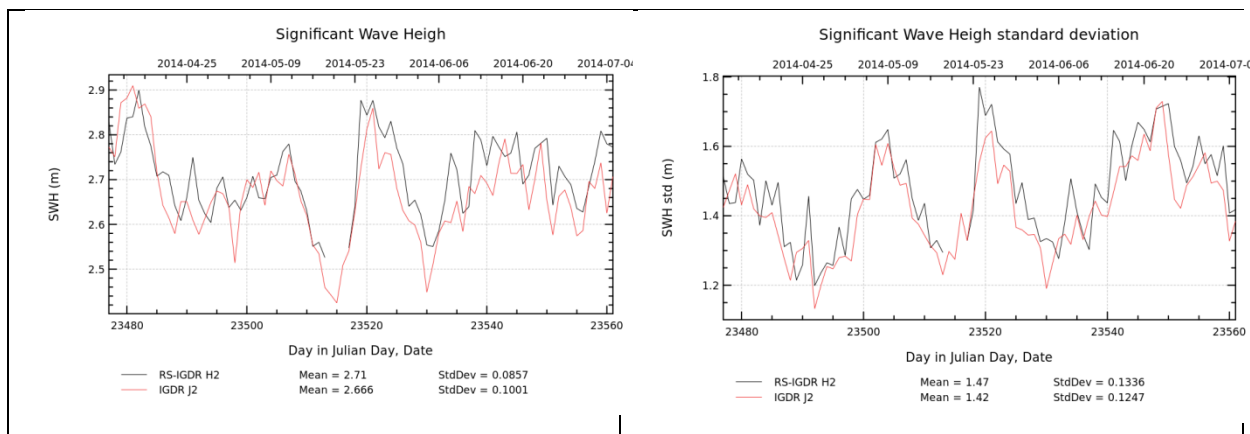


**Figure 8: Temporal evolution of the daily mean (left panel) and standard deviation (right panel) of significant wave height for HY-2A and Jason-2**

The map of SWH differences (Figure 9 left panel) is clearly correlated to the map of HY-2A SWH (Figure 9 right panel). Again HY-2A SWH estimations are impacted by the lack of altimeter instrument calibration data (MLE4 SWH are not corrected from the PTR (Point Target Response) approximation). Few negative values are observed for low SWH, and higher positive values are obtained for high SWH.

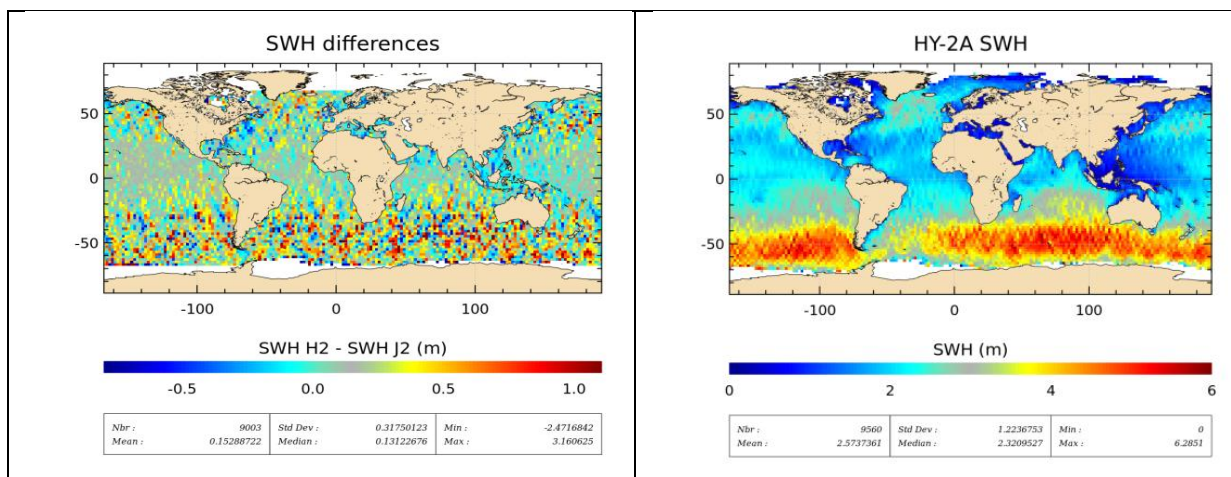


**Figure 9: Map of along track Significant Wave Height differences between HY-2A and Jason-2 over the 3 months available.**

To conclude HY-2A SWH are closed to Jason-2 SWH. As we do not use Look Up Table (LUT) to correct the PTR approximation, differences are correlated with SWH values. These differences could have an impact on the SLA estimation as non corrected SWH are used to compute the one parameter SSB.

### 3.4. Sea State Bias

Concerning the Sea State Bias, the values provided in S-IGDR products were not consistent enough (compared to Jason-2's SSB). Therefore, in a first time, we decided to use a one parameter SSB (depending on SWH only). We estimated it by a basic linear regression of sea level differences at crossovers:  $\Delta SSH = \alpha SWH$  with  $\alpha = -0.034489$ . This simple SSB correction could be improved in the future, as soon as enough HY-2A data is available, to become equivalent to the one applied on Jason missions (no-parametric solution taking into account waves and sigma-0).





Figure 10 displays the improvement provided with the new 1-parameter SSB calculation. The HY-2A's spectral content is closer to Jason-2 spectra.

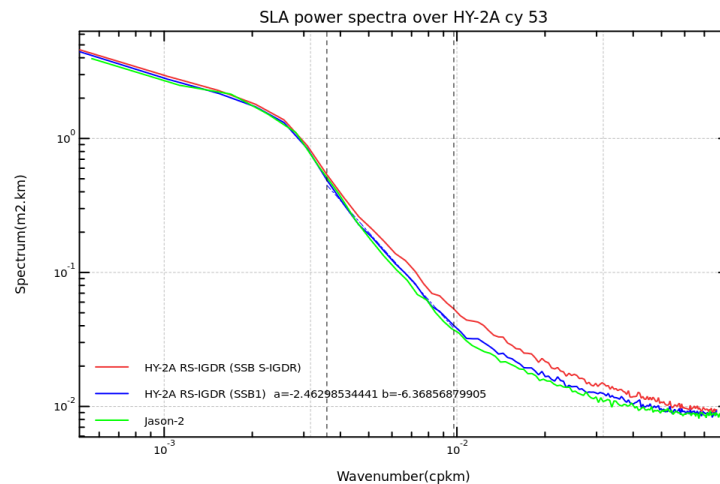


Figure 10: Sea Level Anomaly power spectra computed over HY-2A's cycle 53 with NSOAS SSB (red curve), one parameter SSB (blue curve) and Jason-2 SLA (green curve) computed over the same period.

## 4. Sea level performances

In this section, we analyze the performances of the sea level calculation by analysing the along-track sea level estimations referenced to the mean sea surface (called Sea level Anomalies (SLA)), and by analyzing the Sea Surface Height (SSH) differences at crossovers measurements. To be consistent between both missions, we calculate the Jason-2 SSH and SLA applying the wet troposphere correction and ionosphere correction derived from models (resp. ECMWF and GIM).

### 4.1. Analysis of along-track Sea Level Anomalies

The analysis of the along-track SLA performances is made up of the analysis of high frequency content (spectra analysis), the analysis of correlated geographical biases with Jason-2, and the temporal evolution of SLA in terms of global mean and variance.

#### 4.1.1. High frequency content

To assess the spatial high frequency content of SSH estimation we performed a 20Hz spectra analysis. To not be impacted by geophysical differences or SSB computation differences we compute the spectra analysis with uncorrected SSH. Results presented Figure 11 show that both spectra are very consistent for high and small scales. The 20Hz white noises measured for scales between 700 m and 1.3 km is lower for HY-2A (2.8 cm rms). For wavelengths from 5km to 30km in the spectral hump band we notice slight differences. These discrepancies could be due to altimeter footprint differences (Dibarboure et al, RD 5).

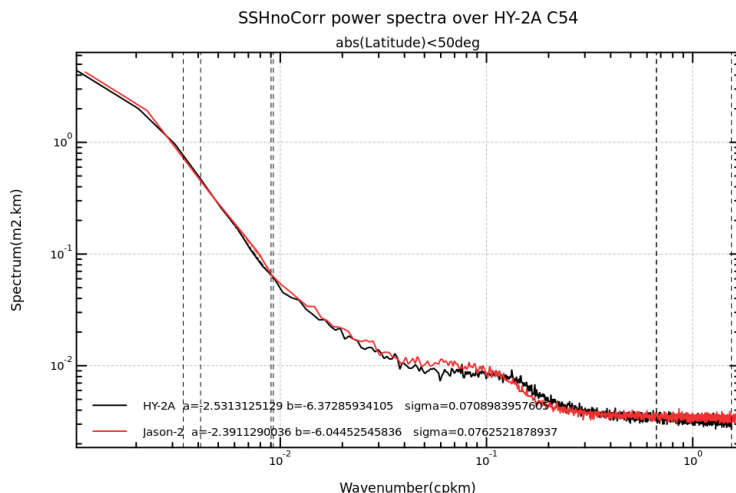


**Figure 11: 20Hz non corrected Sea Surface Height power spectra computed over HY-2A cycle 54 for HY-2A (black curve) and Jason-2 (gray curve)**

To conclude, spectra analysis shows the good agreement on SSH estimations between HY-2A and Jason-2 for high and low wavelength. We also notice the low 20Hz white noise value for HY-2A which traduces the good instrumental performances of the altimeter.

### 4.1.2. Temporal evolution

Looking at the evolution of the global mean of SLA (also called Mean Sea Level - MSL), we have detected a strong negative drift in comparison with Jason-2 (plotted in Figure 12 left panel). The drift value is estimated around -0.1 cm per day (i.e. close to 40 cm per year, inline with other studies). Due to this long term behaviour, we suppose that this is linked to the Ultra Stable Oscillator behaviour not taken into account in the ground processing.

Figure 12 right panel displays the temporal evolution of SLA standard deviation for HY-2A and Jason-2. Very good temporal correlated variations are obtained for both missions, with the HY-2A SLA performance higher than Jason-2 by 2.30 cm rms.

This drift directly impacts SLA estimations and should be monitored. The way it is taken into account is described chapter 5.

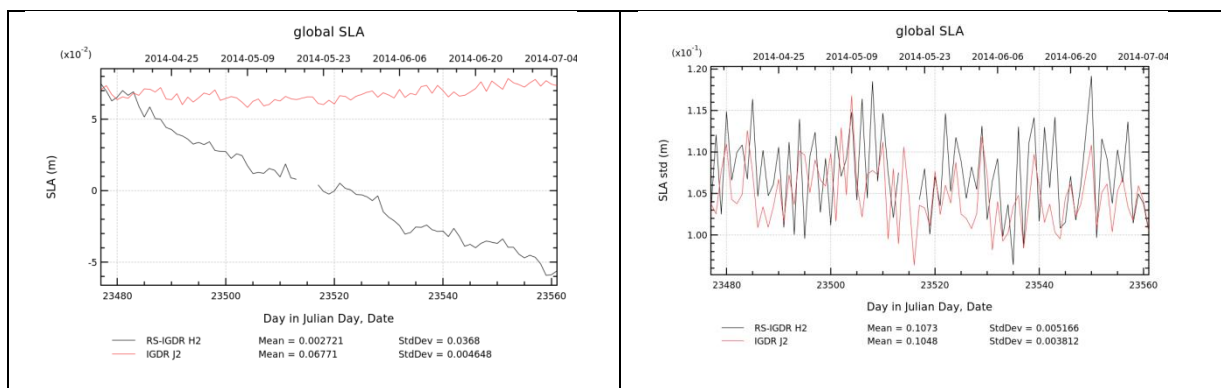


**Figure 12: Temporal evolution of the daily mean (left panel) and standard deviation (right panel) of sea level anomaly for HY-2A and Jason-2. The HY-2A SLA has been align on Jason-2 SLA at the beginning of the time series to facilitate the figure interpretation**





### 4.1.3. Correlated geographical biases with Jason-2

To study geographical correlated biases we performed along track SLA differences with Jason-2. The following map (Figure 13) shows correlated variations of bias as function of longitudes. This result is also observed with multi-mission crossovers diagnosis Figure 18. Similar orders of magnitude are obtained when Cryosat-2 and Jason-2 SLA are compared (Annexe), but in this case the variation seems to be correlated with latitudes.

Geographical biases observed between HY-2A and Jason-2 are quite low. The way they are corrected in DUACS is detailed in chapter 5.

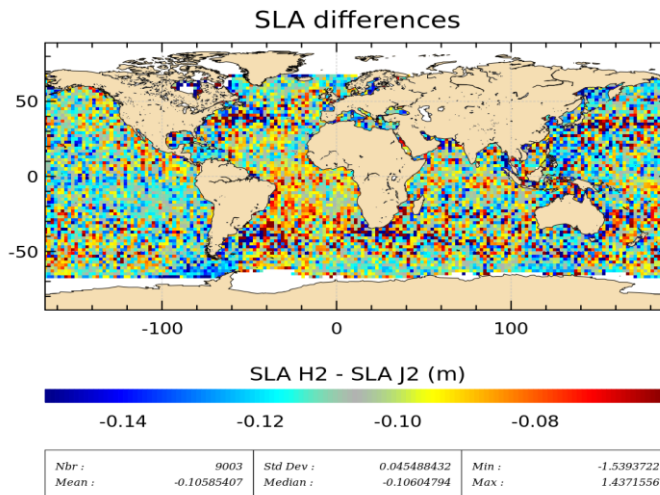


Figure 13: Map of along track Sea Level Anomaly differences between HY-2A and Jason-2 over the 3 months available

## 4.2. Analysis of Sea Surface Height Crossovers Differences

### 4.2.1. Mono mission crossovers

The analysis of SSH differences at crossovers provide a good indicator of the sea level performances.

We compute crossovers applying a selection on time differences shorter than 10 days in order to reduce the effect of oceanic variability. Furthermore, to calculate a reliable indicator geographical selections to remove shallow waters (bathymetry lower than -1000m), high latitudes (above 60°) and high oceanic variability areas are applied.

The standard deviation of SSH differences at crossovers for HY-2A and Jason-2 is compared in Figure 14. HY-2A shows a slightly higher standard deviation at crossovers but overall results are consistent with Cryosat-2 and quite similar with Jason-2 which confirms the good performances of HY-2A altimeter.

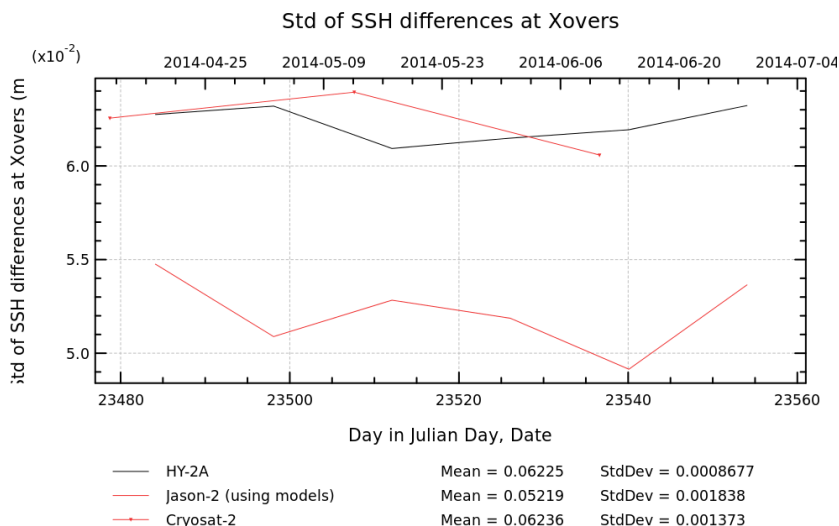


Figure 14: Cycle by cycle standard deviation of the SSH differences at crossovers for HY-2A and Jason-2.

To analyse inconsistencies between ascending and descending passes we compute the mean differences of SSH at crossovers. Figure 15, shows that these differences are low (lower than 1.5 cm) for HY-2A. We also notice that these differences are higher than Jason-2 or Cryosat-2 results.

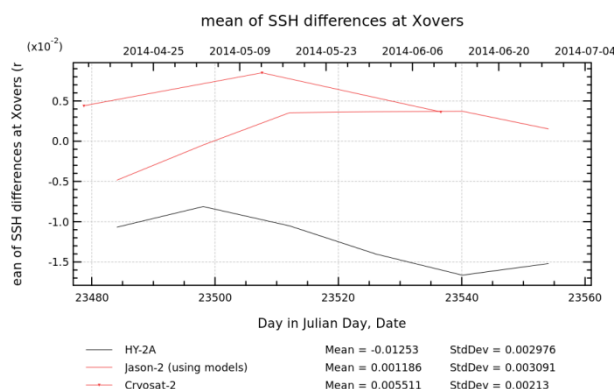


Figure 15: Cycle by cycle mean of SSH differences for HY-2A, Jason-2 and Cryosat-2 mono-mission analyses.

The HY-2A mono-mission crossovers map (Figure 16) shows the spatial distribution of differences between ascending and descending passes. We notice an important contrast between South and North hemispheres with a bias around 1cm for high positive latitudes and -5cm for high negative latitudes. This pattern seems to be correlated with a residual datation bias.

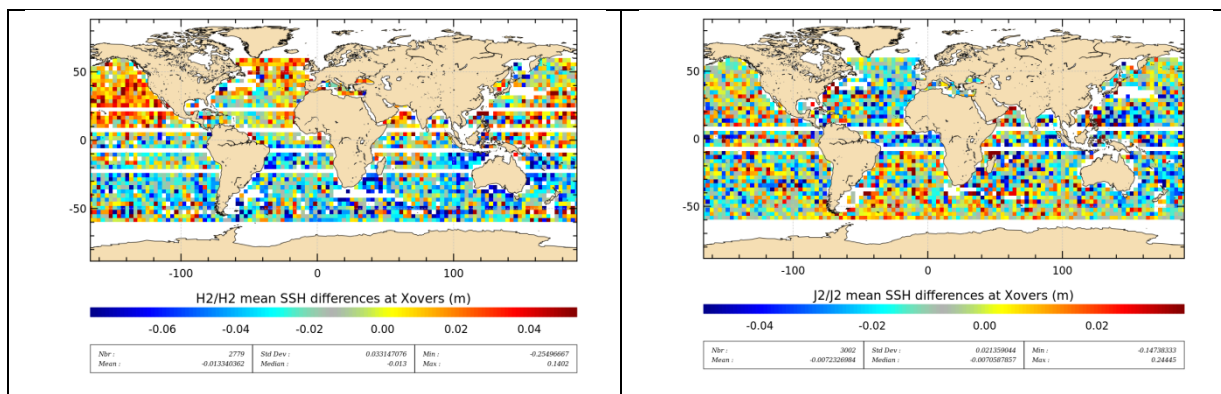


Figure 16: Map of the mean SSH differences at crossovers for HY-2A (left panel) and Jason-2 (right panel) over the 3 months available.

Performing a linear regression between SSH differences and radial velocity at HY-2A mono-mission crossovers we obtained the expression of a residual datation bias:

$$dat_{bias} = -0.000480 * radial\_velocity$$

By taking into account this datation bias (Figure 17), results are much more homogeneous and differences between ascending and descending passes are significantly lower (-2 mm in average against -1.3 cm previously). It means that after applying this correction, the evolution of the daily mean of HY-2A SSH differences at crossovers (black curve presented on Figure 15) is no more centred on -1.3 cm but on -2mm.

This correction has not yet been added in RS-IGDR products, it could generate discrepancies on the order of 1 cm between ascending and descending passes. However it has no impact in DUACS as it is demonstrated in chapter 5.

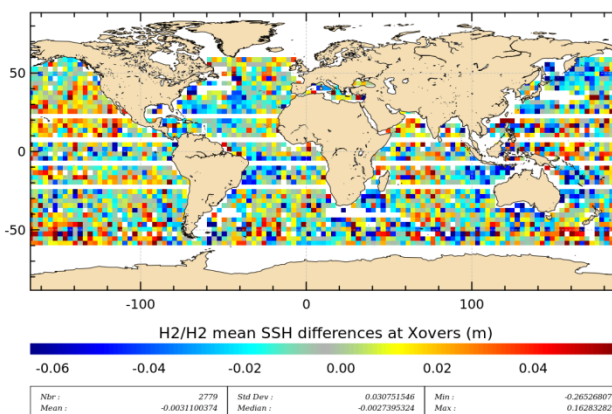


Figure 17: Map of the mean SSH differences at crossovers for HY-2A when datation bias correction is applied

#### 4.2.2. Multi-mission crossovers: HY-2A / Jason-2

Analysing the HY-2A / Jason-2 multi-mission crossovers provides very relevant information on the consistency between both missions since the effect of the oceanic variability is minimized at crossovers. Looking at the mean differences (Figure 18) provide information on the geographical bias observed between HY-2A and Jason-2.



The datation bias determined previously has been applied on HY2 data. Geographical biases are correlated with longitudes. We notice negative differences (around -3cm) in the South-East Pacific and South Indian oceans and low positive differences in Atlantic and West Pacific oceans.

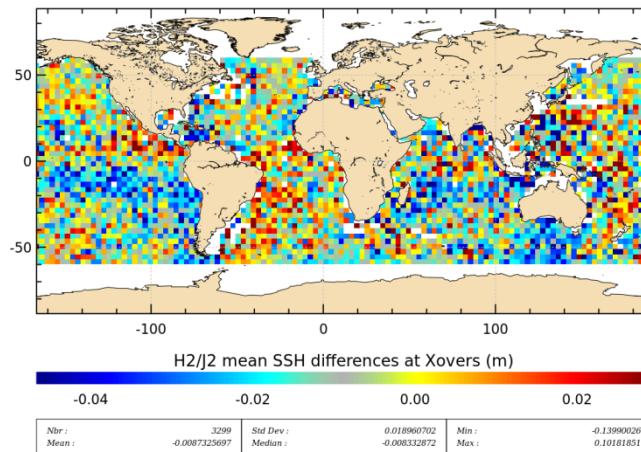


Figure 18: Map of the mean SSH differences between HY-2A and Jason2 at crossovers over the 3 months available.

## 5. Impact in DUACS

HY-2A has been integrated in DUACS at the beginning of June 2014. As Cryosat-2, HY-2A is considered as an opportunity mission. It means that it has less weight than other missions like Jason-2 or AltiKa. To avoid inconsistencies and biases between missions, we take Jason-2 as reference and compute corrections applied on each other missions to be consistent with Jason-2.

This chapter aims at describing HY-2A performances in DUACS using SLA and SSH drifts correction.

### 5.1. Orbit error correction

To remove geographical biases between HY-2A and Jason-2 in DUACS, we compute a long wavelength error based on cubic splines method (F. Mertz et al, RD 4). However in the case of HY-2A, as differences with Jason-2 SLA are high, we firstly perform cycle by cycle global bias correction to roughly adjust HY-2A SLA with Jason-2 and better estimate Orbit Error correction (OE).

### 5.2. Temporal evolution of SLA

The temporal evolution after applying this long scale correction (Figure 19) shows very consistent results between HY-2A and Jason-2. The impact of the USO correction drift is completely removed. We notice that the first values of HY-2A SLA time series are not available or inconsistent, it occurs since the computation of the OE correction need a sufficient number of measurements.

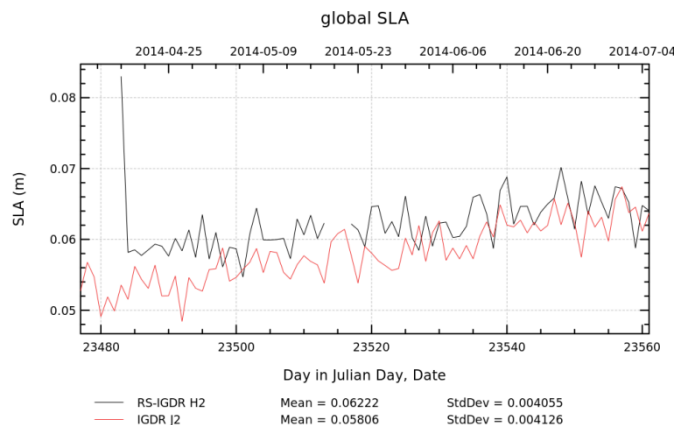


**Figure 19: Temporal evolution of the daily mean (left panel) and standard deviation (right panel) of sea level anomaly for HY-2A and Jason-2.**

### 5.3. Mono-mission crossovers

Analysis of mono-mission crossovers without the OE correction and without the datation bias correction showed in part 4.2.1 highlighted high SSH differences between HY-2A ascending and descending passes. Applying the orbit error, differences showed in Figure 20 are close to 0 cm and do not present important geographical correlated biases except in high oceanic variability area (below  $60^\circ$  south of latitude). It means that the long scale variations due to the datation bias are absorbed by the OE correction.

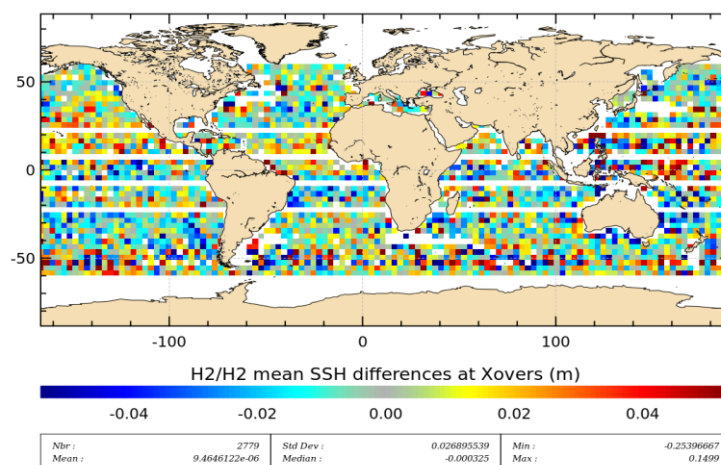


**Figure 20: Map of the mean SSH differences at crossovers for HY-2A over the 3 months available.**

### 5.4. Multi-mission crossovers

First multi-mission crossovers results, computed without the OE correction, showed slight geographical biases correlated with longitudes (section 4.2.2). Applying this correction, differences with Jason-2 at crossovers (Figure 21) are centred in 0cm and their variations are homogeneous over global ocean.

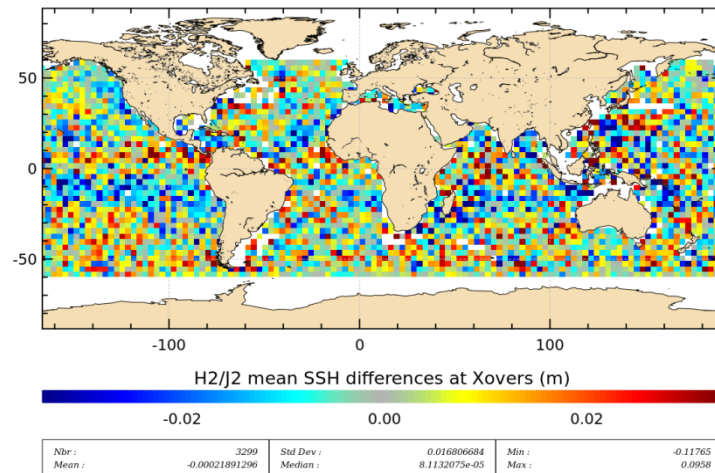


**Figure 21: Map of the mean SSH differences at crossovers between HY-2A and Jason-2 over the 3 months available.**

## 6. Conclusion

After computing a first calibration and validation exercise in January 2014 we demonstrated that HY-2A RS-IGDR data quality fulfils the requirements to be introduced in the DUACS system and thus provides useful information. Based on DUACS dataset this study summarizes the main results of data quality assessment.

We have seen that, over ocean and over land, the number of missing measurements is higher than for Jason-2, in particular for high latitudes. It could be due to a bad positioning of the acquisition windows, and should be managed by the NSOAS. However it doesn't impact the quality of available measurements

The assessment of retracked parameters shows good results, notably for the SWH which is very similar with Jason-2 SWH estimation. The sigma0 distributions are also very close when we apply a bias on HY-2A sigma0. The drift observed on HY-2A sigma0 should be monitored because it could impact our data editing, but once again it doesn't degrade the data quality in the DUACS system.

Number of missing measurements and drifts observed on sigma0 and mispointing are linked to instrumental calibration and cannot be changed in the HPP, it has to be done by the NSOAS in the ground segment.

Analysis of SLA and differences of SSH at crossovers, show the good performances of the HY-2A altimeter. Indeed, as showed by the spectral analysis diagnosis, SSH high frequency content are very consistent for both missions, and the 20Hz white noise is even slightly lower for HY-2A altimeter. Moreover, compared to Jason-2 and for time delay lower than 10 days, SSH estimations at crossovers are consistent and geographical biases are small.

However, we have seen that along track SLA estimations are impacted by an important drift. We suppose that this drift is related to the ultra stable oscillator, and this instrumental correction is not available in NSOAS products. Differences between ascending and descending passes are also observed. We show that these correlated geographical biases are related to an additional datation bias. Nevertheless these negative points have no impact in DUACS system since the OE correction corrects long scale pattern errors.

With a new repetitive ground track and the good quality of RS-IGDR products, HY-2A is a useful opportunity mission for the DUACS system. Despite these good mission performances, technical improvements could be done concerning the SSB (using a non-parametric solution), C band retracking estimates, the computation of Look Up tables, radiometer derived correction... Discussion with Chinese agencies could allow a better understanding of drifts observed.





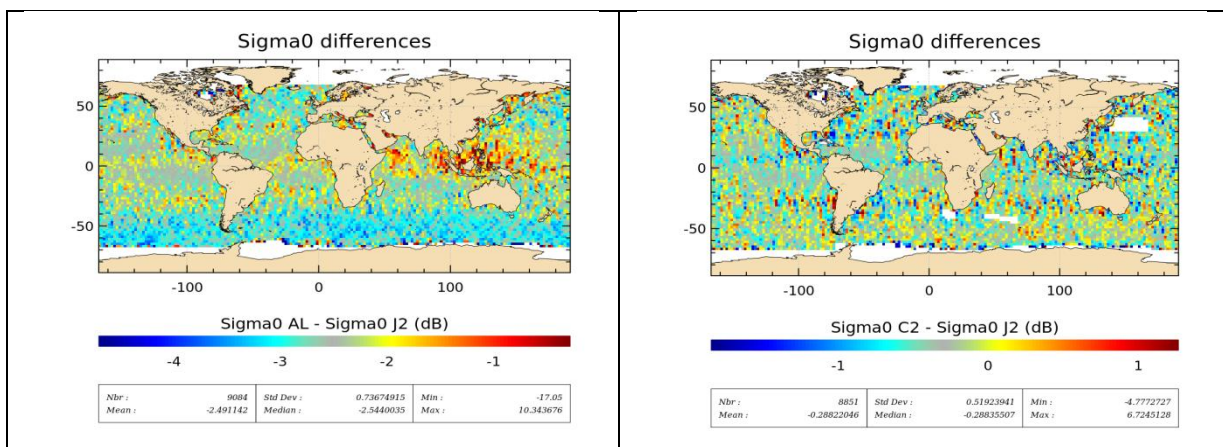
## Appendix A - List of acronyms

CLS	Collecte Localisation Satellites
CNES	Centre National d'Etudes Spatiales
CNSA	China National Space Administration
DUACS	Developing Use of Altimetry for Climate Studies
ECMWF	European Centre for Medium-range Weather Forecasts
GIM	Global Ionosphere Maps
HY-2A	HY-2A Processing Prototype
LUT	Look-Up-Table
MOE	Medium Orbit Ephemeris
NSOAS	National Satellite Ocean Application Service
PTR	Point Target Response
RS-IGDR	Re-processed Sensor Interim Geophysical Data Record
S-IGDR	Sensor Interim Geophysical Data Record
SLA	Sea Level Anomaly
SSB	Sea Surface Bias
SSH	Sea Surface Height
SWH	Significant Wave Height
USO	Ultra Stable Oscillator

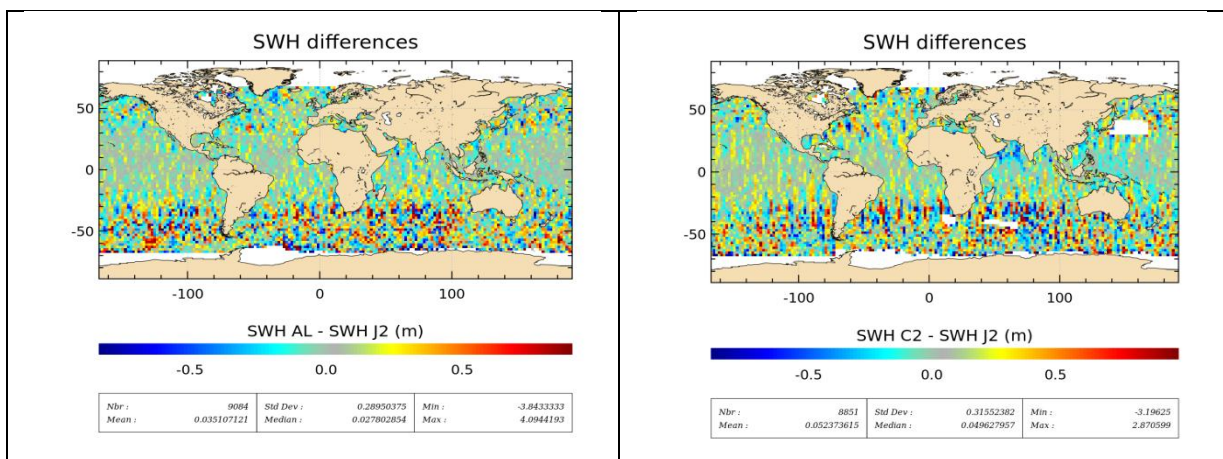




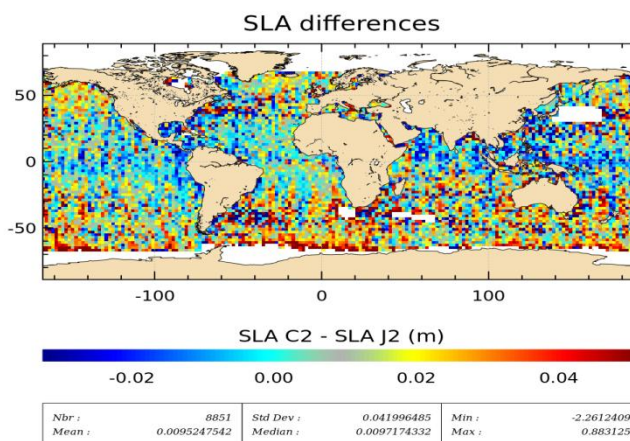
Appendix B - ANNEXES



Map of along track Sigma0 differences between HY-2A and Jason-2 over the 3 months available



Map of along track Significant Wave Height differences between HY-2A and Jason-2 over the 3 months available.



Map of along track Sea Level Anomaly differences between HY-2A and Jason-2 over the 3 months available

Proprietary information: no part of this document may be reproduced divulged or used in any form without prior permission from CNES.